AGU PUBLICATIONS

JGR

Journal of Geophysical Research: Atmospheres

RESEARCH ARTICLE

10.1002/2014JD022098

Key Points:
- Definition of a new Heat Wave Magnitude Index
- Classification of the magnitude of the heat waves occurred in the present
- Prediction of heat wave magnitude under climate scenarios

Correspondence to:
S. Russo,
simone.russo@jrc.ec.europa.eu

Citation:
Russo, S., A. Dosio, R. G. Graversen, J. Sillmann, H. Carrao, M. B. Dunbar, A. Singleton, P. Montagna, P. Barbola, and J. V. Vogt (2014), Magnitude of extreme heat waves in present climate and their projection in a warming world, *J. Geophys. Res. Atmos.*, *119*, 12,500–12,512, doi:10.1002/2014JD022098.

Received 3 JUN 2014
Accepted 19 OCT 2014
Accepted article online 24 OCT 2014
Published online 20 NOV 2014

Magnitude of extreme heat waves in present climate and their projection in a warming world

Simone Russo[1,2], Alessandro Dosio[1], Rune G. Graversen[3], Jana Sillmann[4], Hugo Carrao[1], Martha B. Dunbar[1], Andrew Singleton[5], Paolo Montagna[6], Paulo Barbola[1], and Jürgen V. Vogt[1]

[1]European Commission, Joint Research Centre, Ispra, Italy, [2]Institute for Environmental Protection and Research, Rome, Italy, [3]Department of Physics and Technology, University of Tromsø, Tromsø, Norway, [4]Center for International Climate and Environmental Research, Oslo, Norway, [5]Norwegian Meteorological Institute, Oslo, Norway, [6]Istituto di Scienze Marine, Centro Nazionale delle Ricerche, Bologna, Italy

Abstract An extreme heat wave occurred in Russia in the summer of 2010. It had serious impacts on humans and natural ecosystems, it was the strongest recorded globally in recent decades and exceeded in amplitude and spatial extent the previous hottest European summer in 2003. Earlier studies have not succeeded in comparing the magnitude of heat waves across continents and in time. This study introduces a new Heat Wave Magnitude Index that can be compared over space and time. The index is based on the analysis of daily maximum temperature in order to classify the strongest heat waves that occurred worldwide during the three study periods 1980–1990, 1991–2001, and 2002–2012. In addition, multimodel ensemble outputs from the Coupled Model Intercomparison Project Phase 5 are used to project future occurrence and severity of heat waves, under different Representative Concentration Pathways, adopted by the Intergovernmental Panel on Climate Change for its Fifth Assessment Report (AR5). Results show that the percentage of global area affected by heat waves has increased in recent decades. Moreover, model predictions reveal an increase in the probability of occurrence of extreme and very extreme heat waves in the coming years, in particular, by the end of this century, under the most severe IPCC AR5 scenario, events of the same severity as that in Russia in the summer of 2010 will become the norm and are projected to occur as often as every 2 years for regions such as southern Europe, North America, South America, Africa, and Indonesia.

1. Introduction

In a future warmer climate with increasing mean temperatures, heat waves will not only become more frequent; their duration and intensity are very likely to increase as well [*Min et al.*, 2011; *Intergovernmental Panel on Climate Change*, 2012; *Coumou and Rahmstorf*, 2012]. In the past few years several climate indices have been applied in order to quantify the heat wave duration and severity based on nighttime minima or daytime maxima [*Perkins and Alexander*, 2012; *Frich et al.*, 2002; *Kiktev et al.*, 2003; *Schär et al.*, 2004; *Meehl and Tebaldi*, 2004; *Alexander et al.*, 2006; *Orlowsky and Seneviratne*, 2011; *Russo and Sterl*, 2011; *Sillmann et al.*, 2013a]. However, all of these indices have been found to have a limited robustness when applied for comparing the severity of heat waves across regions and time [*Otto et al.*, 2012; *Perkins and Alexander*, 2012]. Most of the defined heat wave indices tend to be constructed with a certain impact group or sector in mind (e.g., human health, wildlife, agriculture, bushfire-wildfire, management, transport, and electricity and power) and, due to their complexity, may not be transferable across regions nor between groups, nor across time periods [*Perkins and Alexander*, 2012]. The Heat Wave Duration Index defined by *Frich et al.* [2002], which is one of the first proposed indices used to detect the impact of heat waves, is found to be statistically unrobust [*Kiktev et al.*, 2003; *Alexander et al.*, 2006; *Russo and Sterl*, 2011]. This is because *Frich et al.* [2002] used a fixed threshold of 5°C above climatology to compute the index. This threshold is too high in many regions, such as the tropics, where the variability of daily maximum temperature is low. To overcome this problem, the Expert Team on Climate Change Detection and Indices (ETCCDI; see http://etccdi.pacificclimate.org/list_27_indices.shtml) replaced this index with the Warm Spell Duration Index (WSDI) which is calculated using a percentile-based threshold. The WSDI is able to improve the spatial intercomparability of heat wave duration, but it appears to have some limitations as well. It is calculated for seasons and years individually, which means that heat waves, occurring across two different seasons, are split into two [*Orlowsky and Seneviratne*, 2011; *Intergovernmental Panel on Climate Change*, 2012].

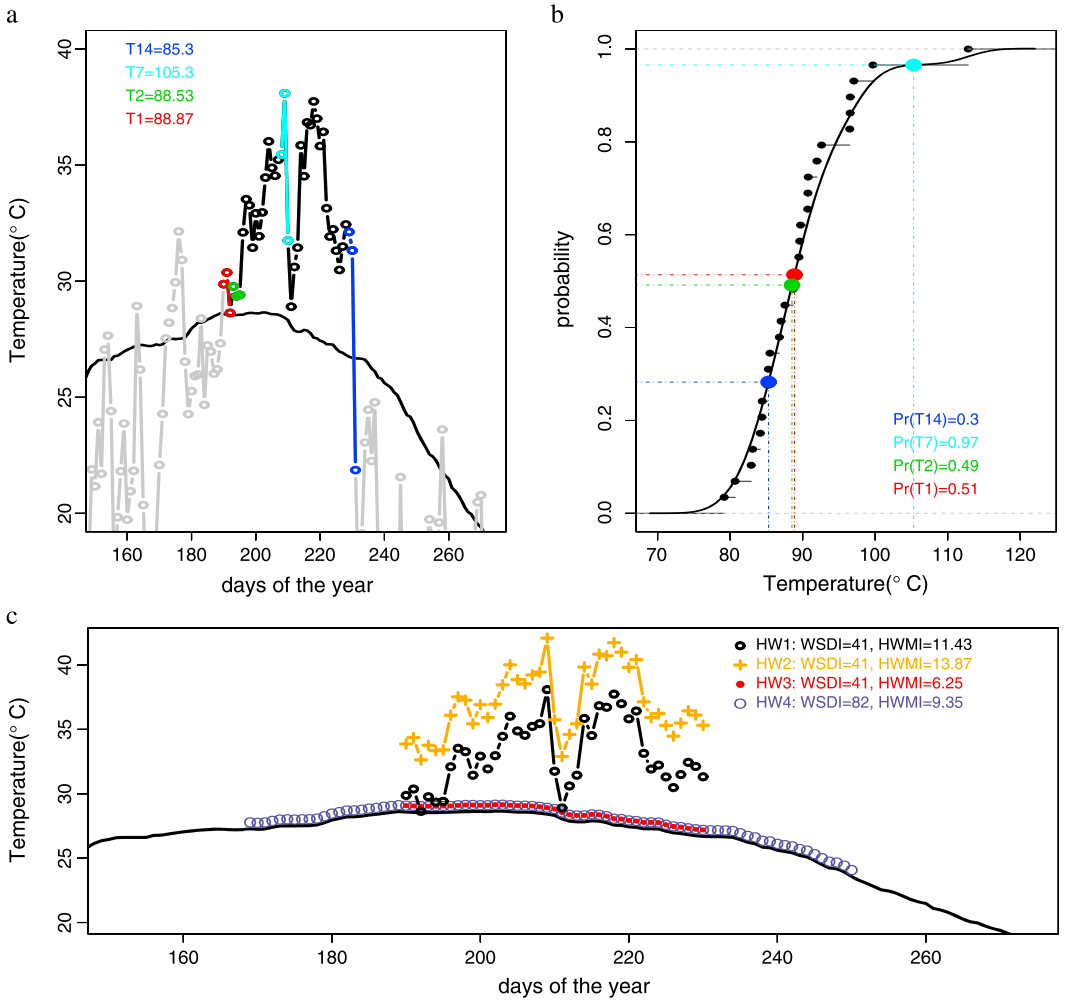

Figure 1. HWMI estimation: calculation scheme example for the 2010 heat wave in Russia. (a) ERA-I time series of the year 2010 of daily maximum temperature in Russia (open circles joined by gray and black lines) and daily threshold (black line). The open circles that are not in gray represent the daily maximum temperature values of the 2010 Russia heat wave. They constitute 14 subheat waves (four of these, selected arbitrarily, are represented by red, green, cyan, and blue open circles). (b) Empirical distribution of the sum of the three highest consecutive daily maximum temperatures of each year within the reference period 1981–2010 (black points) fitted by means of the kernel density estimator (see section S2) in order to obtain the empirical cumulative distribution function (black line). (c) WSDI and HWMI calculated for the Russian heat wave in 2010 and for three different conceptual types of heat wave defined for comparisons (see section 2.4).

In addition, the WSDI takes into account only the duration of a heat wave, meaning that two heat waves of the same length will be considered equally severe even if one of these has higher temperature values than the other. This study presents an alternative index called Heat Wave Magnitude Index (HWMI) that can be compared across regions and time and that takes into account both magnitude and duration of the heat waves. Based on this index, heat waves in the projected future climate can be compared with those of today.

2. Materials and Methods

2.1. Heat Wave Magnitude Index

The Heat Wave Magnitude Index is defined as the maximum magnitude of the heat waves in a year, where heat wave is the period $\geq$ 3 consecutive days with maximum temperature above the daily threshold for the reference period 1981–2010. The threshold is defined as the 90th percentile of daily maxima, centered on a

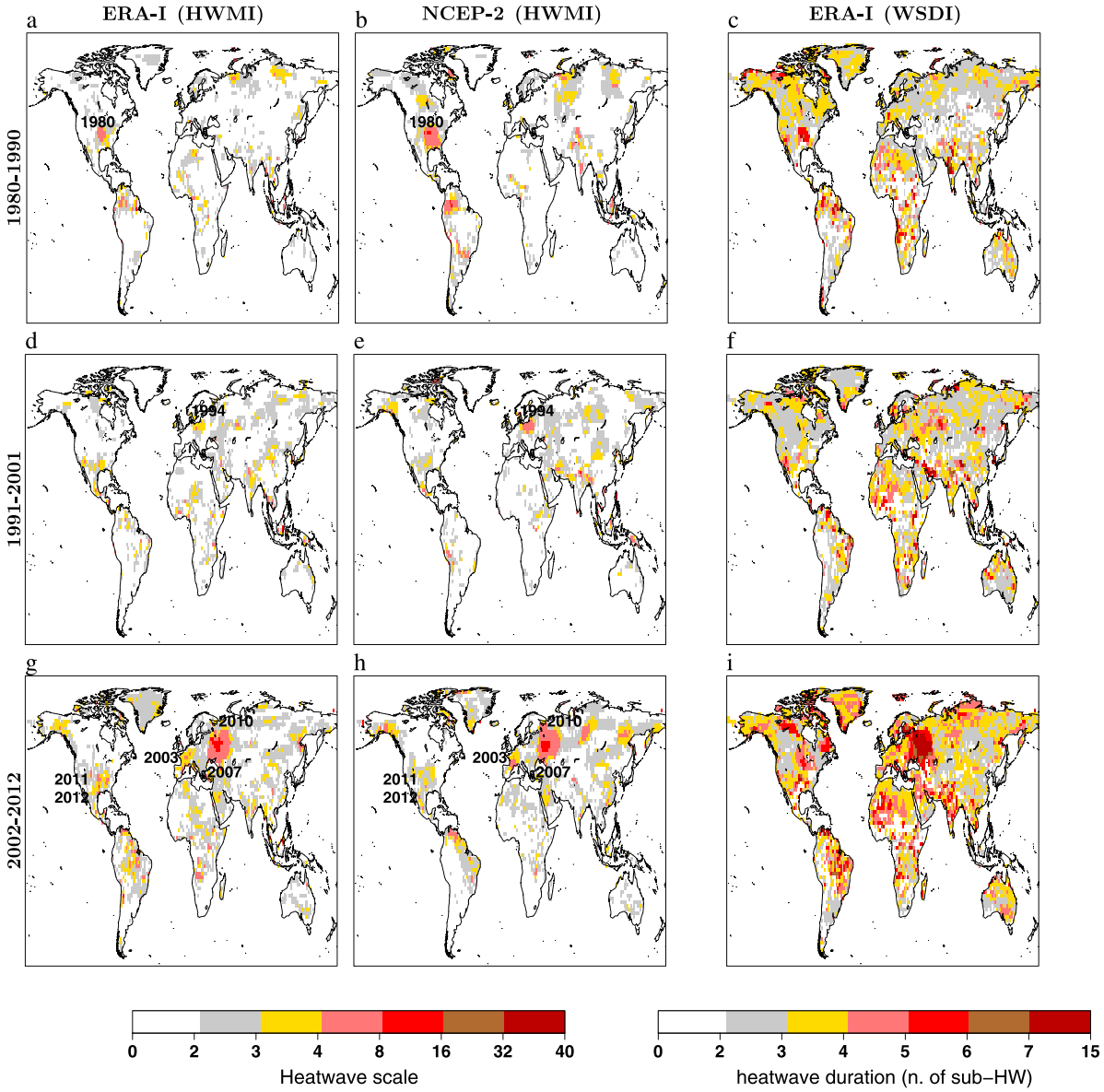

Figure 2. Heat Wave Magnitude Index and Warm Spell Duration Index in three periods of 11 years with reanalysis data: (a–c) 1980–1990, (d–f) 1991–2001, and (g–i) 2002–2012. The WSDI values are expressed as number of subheat waves calculated as WSDI/3.

31 day window. Hence, for a given day d, the threshold is the 90th percentile of the set of data A_d defined by

$$A_d = \bigcup_{y=1981}^{2010} \bigcup_{i=d-15}^{d+15} T_{y,i}, \tag{1}$$

where $\bigcup$ denotes the union of sets and $T_{y,i}$ is the daily maximum temperature of the day i in the year y.

The minimum number of consecutive hot days required to be considered as heat wave may vary across regions: for example, *Perkins and Alexander* [2012], focusing on Australia, have defined a heat wave as an event of at least three consecutive days above threshold, whereas *Fischer and Schär* [2010] defined a European heat wave as an event of at least 6 days duration.

Since we are focusing on a global scale, we have chosen the definition of 3 days for a heat wave. Had we defined a heat wave as a minimum of 6 days, the 3 day heat waves would be excluded, whereas the 3 day definition does not exclude the possibility of detecting longer heat waves.

2.2. HWMI Calculation

The HWMI computation for a specific year is a multiple stage process explained below. As an example, the computations are shown for a ERA-Interim (ERA-I; see section 2.5) grid point (longitude = 35.625°E, latitude = 56.89°N in Figure 1), where the 2010 Russian heat wave shows its maximum value:

1. *Daily threshold*. By using the above definition, a daily threshold is calculated for the reference period 1981–2010 (Figure 1a, black curve).
2. *Heat wave selection*. For each specific year we select all the heat waves composed of at least three consecutive days with daily maximum temperature above the daily threshold. For the selected grid point the length of the detected heat wave in 2010 is 41 days (Figure 1a).
3. *Heat wave to subheat waves*. Each heat wave is then decomposed into *n* subheat waves, where a subheat wave is a heat wave of three consecutive days. For the selected grid point we obtain 13 subheat waves for a total of 39 days; in order to give weighting to the last 2 days of the heat wave, these are grouped with the consecutive day value below the threshold (Figure 1a). In general, in case a heat wave has a length which is not a multiple of 3 days, the last days (one or two) of the heat wave are grouped into a subheat wave with consecutive days below the threshold so that the last subheat wave of the heat wave includes 3 days as well.
4. *Subheat wave unscaled magnitude*. The sum of the three daily maximum temperatures of a subheat wave.
5. *Subheat wave magnitude*. The subheat wave unscaled magnitude is transformed into a probability value on a scale from 0 to 1 (see section 2.3), which is defined as the magnitude of a subheat wave (Figure 1).
6. *Heat wave magnitude*. The magnitude of each heat wave is defined as the sum of the magnitudes of the n subheat waves.
7. *Heat wave magnitude index*. The maximum of all heat wave magnitudes for a given year.

2.3. Estimation of Subheat Wave Magnitude

The computation of the magnitude of a subheat wave is a two-stage process: (1) An empirical (nonparametric) cumulative density function (ECDF) is fitted to the annual maximum of the subheat wave unscaled magnitudes within the reference period 1981–2010 (see Figure 1b and Appendix A) and (2) the magnitude of a subheat wave is a probability value between 0 and 1 estimated from the subheat wave unscaled magnitude using the cumulative density function obtained in the previous stage (see Figure 1).

2.4. Robustness of the HWMI Versus Other Indices

In a recent study, *Perkins and Alexander* [2012] discussed the limitations of most of the ETCCDI extreme temperature indices with regard to the detection of heat wave events. In general, these indices take into account only one single aspect (i.e., maximum temperature, duration, or frequency) during a defined period, which is not necessarily part of a heat spell. This is the case, for instance, of the TX90p index (see http://etccdi.pacificclimate.org/list_27_indices.shtml) measuring the percentage of days with daily maximum temperature above the 90th percentile threshold (see section 2). Only the WSDI, used by ETCCDI, has been specifically defined for detecting heat spells, but it considers only the duration of a heat wave: as a result, two heat waves of the same length are considered equally severe, even if all the days of one had higher (or lower) temperatures than the other."

In order to clarify this further, we compare the WSDI and HWMI calculated for the Russian heat wave in 2010 at the selected grid point (HW1, Figure 1c) with those of three different conceptual types of heat wave (Figure 1c, HW2, HW3, and HW4) with daily temperature values defined as follows: *HW*2 = HW1 temperature values + 4°C, *HW*3 = threshold temperature values from day 190 to 230 + 0.5°C, and *HW*4 = threshold temperature values from day 169 to 250 + 0.5°C.

The heat waves HW2 and HW3 are the same length as the HW1, whereas the HW4 length is double than that of the HW1. Therefore, the HW2 and HW3 are two examples of heat waves of the same duration but with different magnitudes.

If the temperature of all the days of the HW1 increases by 4°C, then we will have a heat wave of type HW2, with the same WSDI as HW1 but greater HWMI. In contrast, an event of the type HW3 is an example of a heat wave with WSDI value equal to that of HW1 but lower magnitude, corresponding to a HWMI value of about 50% lower than the magnitude of HW1. Finally, the HW4 heat wave represents the case of a heat wave twice the duration of the Russian heat wave but lower magnitude.

Table 1. List of Record-Breaking Heat Wave Events in the Period 1980–2012[a]

	U.S. (1980)	Benelux (1994)	Europe (2003)	Greece (2007)	Russia (2010)	U.S. (2011)	U.S. (2012)
				NCEP-II			
Grid points	91	61	51	61	148	38	53
Max	8.20	5.49	4.70	3.76	11.71	4.17	3.75
Mean	4.65	3.26	3.30	2.46	5.50	2.72	2.71
Median	4.10	2.91	3.48	2.36	5.43	2.57	2.60
				ERA-I			
Grid points	54	37	47	78	148	44	55
Max	5.51	4.30	6.26	4.02	11.43	10.44	5.56
Mean	3.46	3.01	3.53	2.58	5.37	3.51	2.96
Median	3.23	3.05	3.72	2.51	5.29	3.14	2.76

[a]The spatial extension is estimated by counting the grid points within a specific event with HWMI equal to or greater than 2.

2.5. Models and Reanalysis

Daily maximum temperature data from the ERA-Interim (ERA-I) reanalysis from European Centre for Medium-Range Weather Forecasts [*Dee et al.*, 2011] and National Centers for Environmental Prediction-Department of Energy Reanalysis-2 (NCEP-2) [*Kanamitsu et al.*, 2002] are applied to study heat waves in the present climate. Both data sets have a 6-hourly time resolution and are available from 1979 onward. The ERA-I is based on a T255 resolution (~79 km); however, the data are truncated to T63 for comparison with the NCEP-2 and model data.

For future projections, daily maximum temperatures from 16 model simulations were obtained from the Coupled Model Intercomparison Project Phase 5 (CMIP5) archive (see Appendix Table C1). The HWMI was calculated for the period 2006–2100 for all models under three different scenarios (i.e., Representative Concentration Pathway 2.6 (RCP2.6), RCP4.5, and RCP8.5), described by *Taylor et al.* [2012] as follows:

RCP2.6. The radiative forcing reaches a maximum near the middle of the 21st century before decreasing to an eventual nominal level of 2.6 W m^{-2} by the end of the century.
RCP4.5. The radiative forcing increases until the middle of the 21st century before stabilizing to a level of 4.5 W m^{-2} by the end of the century.
RCP8.5. The radiative forcing increases throughout the 21st century before reaching a level of about 8.5 W m^{-2} by the end of the century.

For the period between 1980 and 2005 historical model simulations were used [*Taylor et al.*, 2012]. We used the period 1980–2012 for a comparison with the reanalysis.

All CMIP5 models and reanalysis data were interpolated onto the same T63 grid (1.875 × 1.875°).

2.6. Uncertainties of the Ensemble Models

The spread of the ensemble models has been estimated as the annual interquartile range (IQR) of the 16 HWMI global and regional medians (see Figure 3). The IQR is defined as the difference between the third (Q3) and the first (Q1) quartiles of the set of data [*Rousseeuw and Leroy*, 1987]. In robust statistics, a value is defined as outlier if it is outside of the interval $[Q1 - 1.5IQR, Q3 + 1.5IQR]$.

3. Results

In this study the heat wave magnitudes have been classified according to a new scale defined in Appendix B for values of the HWMI with the following categories:

≤ 1 Normal $< 2 \leq$ Moderate $< 3 \leq$ Severe $< 4 \leq$ Extreme $< 8 \leq$ Very Extreme $< 16 \leq$ Super Extreme $< 32 \leq$ Ultra Extreme.

In the 11 years between 2002 and 2012, the percentage of global area affected by moderate (HWMI $\geq$ 2), severe (HWMI $\geq$ 3), and extreme (HWMI $\geq$ 4) heat waves was threefold greater than in the previous periods (1980–1990 and 1991–2001). This is evident from Figure 2 showing the geographical pattern of the

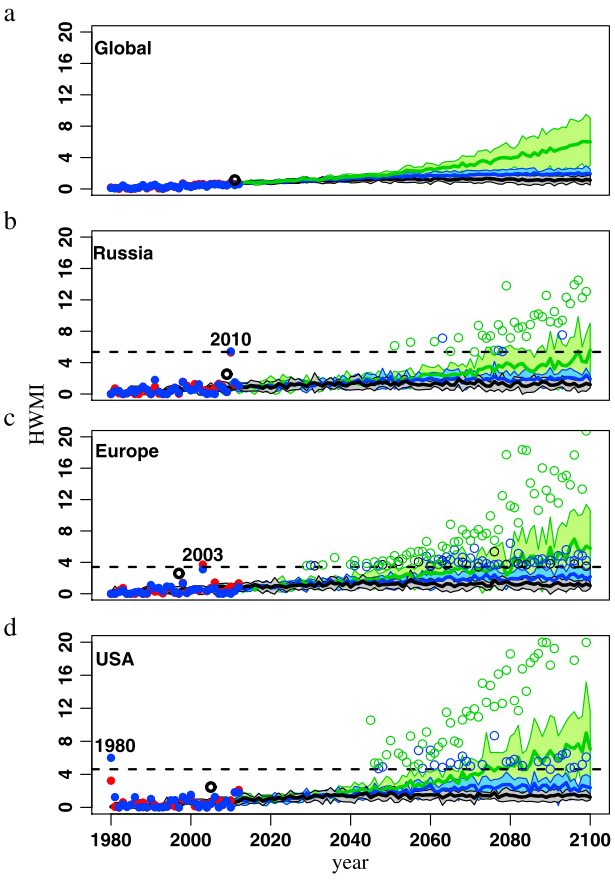

Figure 3. Global and regional median time series of the HWMI relative to 1980–2100. (a) Global median: Blue and red points correspond to the HWMI values with the NCEP-II and ERA-Interim data, respectively. The open black circle is the maximum HWMI value of the 16 models within the present period 1980–2012. Black, blue, and green lines denote the CMIP5 multimodel ensemble median, respectively, for the RCP2.6, RCP4.5, and RCP8.5 scenarios. Gray, green, and light blue shaded areas denote the annual interquartile range (see section 2) of the multimodel ensemble, respectively, for the RCP2.6, RCP4.5, and RCP8.5 scenarios. (b–d) As Figure 3a but for the three regions affected by the Russia (2010), Central Europe (2003), and the U.S. (1980) heat waves. Black, blue, and green open circles in the future period denote the HWMI of the model ensemble represented only if the value is greater than or equal to the HWMI value of the 2010, 2003, and 1980 (dashed black lines).

maximum HWMI, from the ERA-I and NCEP-2 data, within three periods: 1980–1990, 1991–2001, and 2002–2012. A list of the most severe heat waves that occurred in the period 1980–2012 is presented in Table 1.

The 2010 Russian heat wave shows the highest HWMI value and the largest extension with both the ERA-interim and NCEP-2 data sets. In particular, the 2010 Russian heat wave shows a spatial extension nearly 3 times larger and with a maximum HWMI approximately double that of the heat wave in Europe in 2003 (see Table 1). Qualitatively similar conclusions were found in a recent study [*Barriopedro et al.*, 2011] providing evidence that the anomalous 2010 heat wave exceeded the amplitude and spatial extent of the 2003 European summer heat wave. Additional record-breaking European heat waves occurred in 1994 and 2007 in Germany-Benelux and Greece, respectively. According to the HWMI values calculated from reanalysis data, the regional mean and median of both these events were, however, less severe than the 2003 heat wave (see Table 1).

Another extreme heat wave, albeit less frequently studied in the literature, occurred in the U.S. in 1980. According to the NCEP-2 reanalysis, the 1980 U.S. heat wave can be considered the second strongest in the period 1980–2012, whereas the ERA-I data show that this event was of comparable magnitude as the 2003 European heat wave (see Table 1). Two other important heat waves occurred in the U.S. in the years 2011 and 2012 with HWMI values comparable to the 1994 and 2007 events in Germany-Benelux and Greece, respectively (see Table 1).

It must be noted that this comparison of heat wave strengths based on HWMI cannot be performed with the WSDI as it takes into account only the duration of a heat wave. In fact, there are many events that occurred in the last 33 years in different regions, such as North America, Greenland, northern West Africa, and southeast Australia, of long duration resulting in WSDI values comparable to those of the 2003 European heat wave (Figure 2, right-hand frames). However, those events show lower HWMI values than that in Europe 2003; although they were of long duration, the temperature anomalies associated with these events were smaller than those of the Europe 2003 heat wave.

In order to evaluate whether general circulation models (GCMs) are capable of reproducing the intensity and frequency of heat waves in the present climate, as well as to quantify their changes in a future warmer

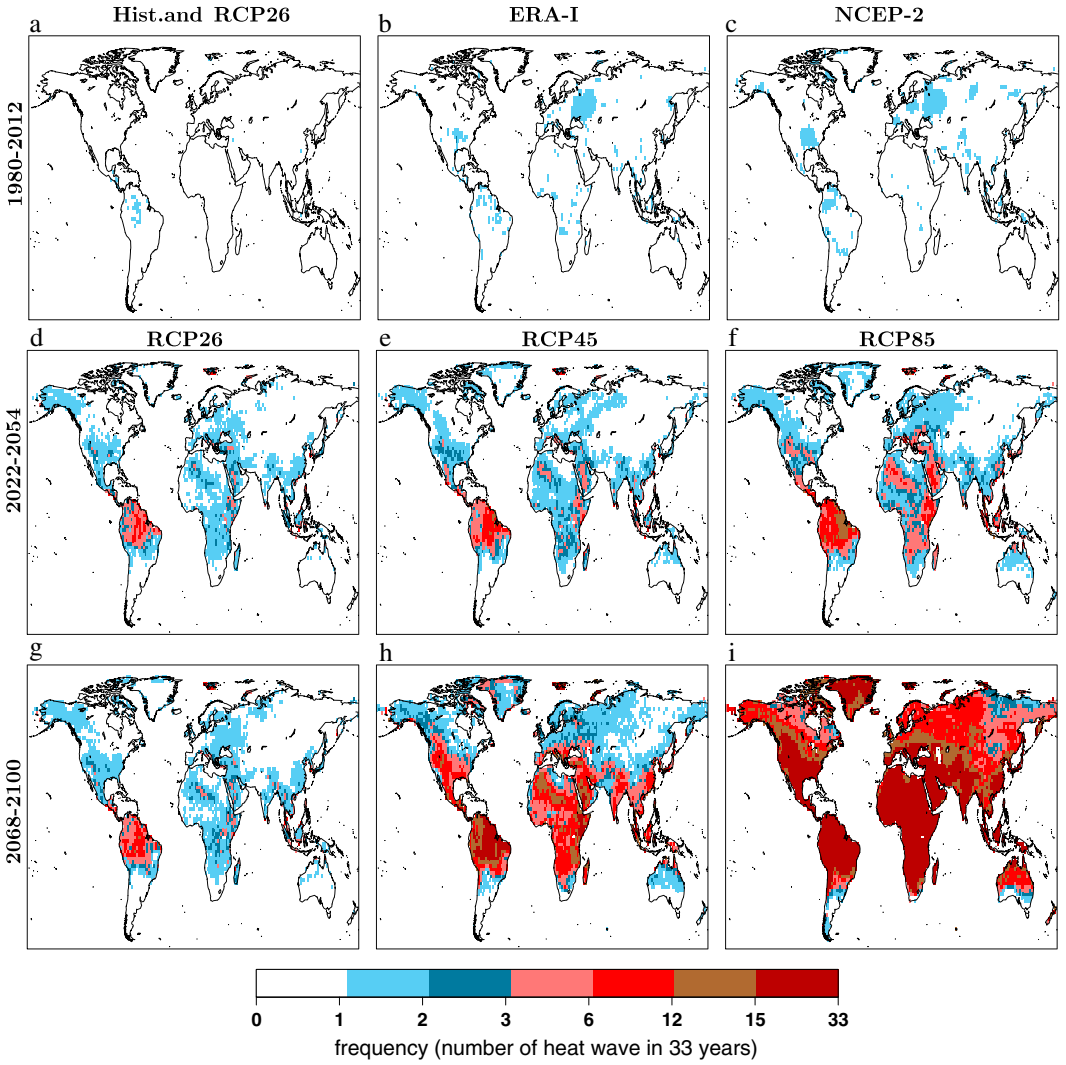

Figure 4. Number of extreme heat waves (HWMI ≥ 4) in present and future climate. (a) Historical (1980–2005) and RCP2.6 scenario (2006–2012) for the multimodel CMIP5 ensemble, (b) ERA-Interim, (c) NCEP-2, (d–f) median of the number of heat waves of the multimodel ensemble in the near future (2020–2052) under the RCP2.6, RCP4.5, and RCP8.5 scenarios, respectively. (g–i) As Figures 4d–4f but for the future period (2068–2100).

climate, we estimated the spatial median of the HWMI of the entire globe and of three subregions, the U.S., Europe, and Russia, composed of those grid points with HWMI values (calculated using ERA-I) equal to or greater than 2 during the strongest events in 1980, 2003, and 2010, respectively (see Figure 3 and Table 1).

GCMs HWMI values for the period 1980–2012 were compared with those calculated from the ERA-I and NCEP-2 reanalysis data. The global and regional yearly evolution of the HWMI model ensemble medians does not differ significantly from those estimated with the reanalysis data sets (Figure 3). The significance is based on the 1% level of a Kolmogorov-Smirnov test. Moreover, the significant positive HWMI global median trends estimated with the models are very similar to those estimated with reanalysis data (see Appendix Table D1).

At regional scale, however, models show limitations in simulating single extreme heat wave events. In particular, for the period 1980–2012 in Russia, the maximum HWMI value of the 16 models (HWMI = 2) differs significantly from the regional HWMI median calculated with ERA-I and NCEP-2 reanalysis (HWMI = 5.43 and 5.29, respectively; see Figure 3b). From a statistical point of view, the events that occurred in 2010 (Russia), 2003 (Europe), and 1980 (U.S.) can be considered outliers, rare events, or extremes [*Gumbel*, 1954; *Rousseeuw*

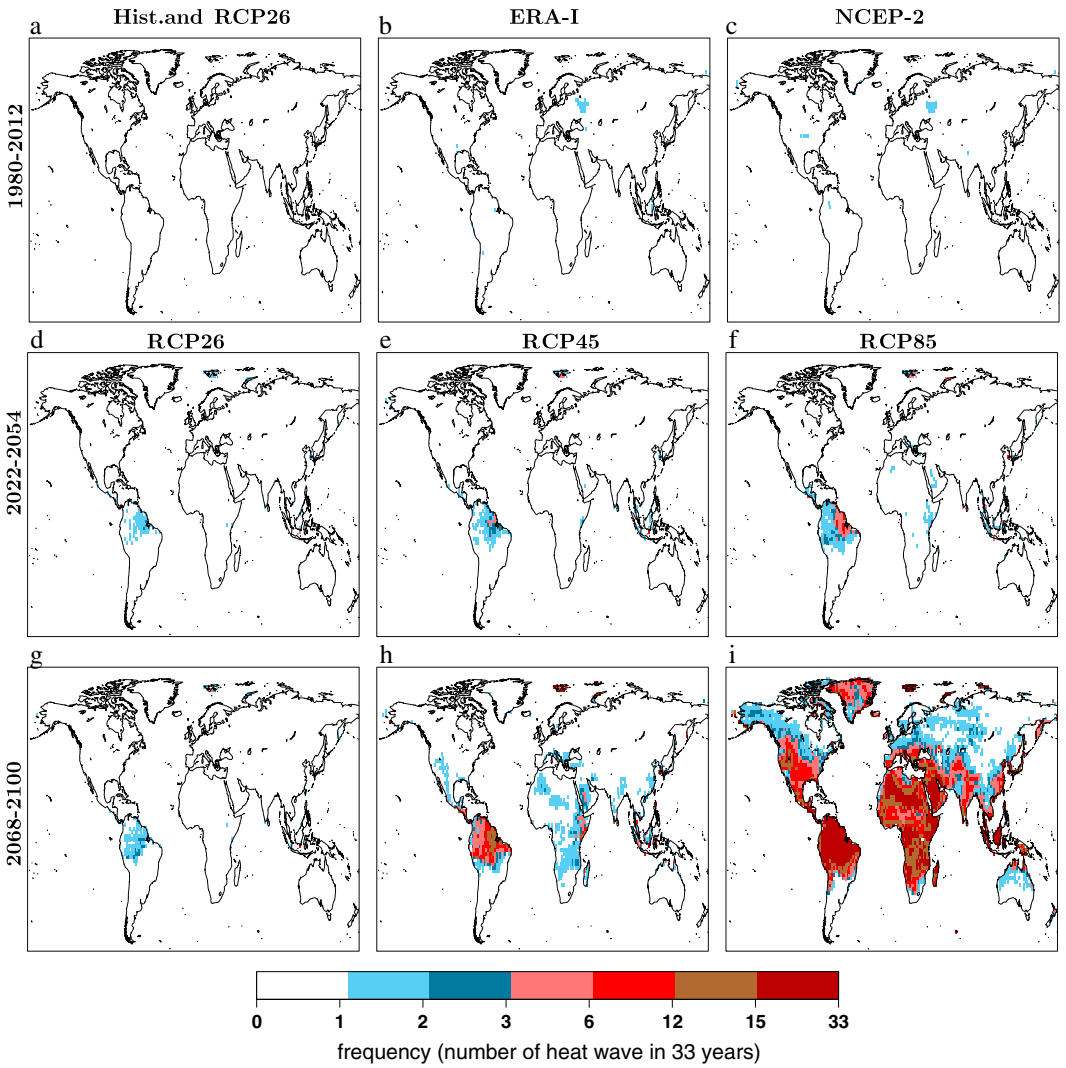

Figure 5. Number of very extreme heat waves (HWMI $\geq$ 8) in present and future climate. (a) Historical (1980–2005) and RCP2.6 scenario (2006–2012) for the multimodel CMIP5 ensemble, (b) NCEP-2, (c) ERA-Interim, and (d–f) median of the number of heat waves of the multimodel ensemble in the near future (2020–2052) under the RCP2.6, RCP4.5, and RCP8.5 scenarios, respectively. (g–i) As Figures 5d–5f but for the future period (2068–2100).

and Leroy, 1987] (Figures 3b–3d and section 2.6). Similar considerations can be done for the other severe heat waves listed in Table 1, recording a maximum HWMI value of the 16 models in general lower than 2.5.

In a warming world with a significant positive temperature trend, all the models show an increase of the HWMI global median in the near future (2020–2052) for all the RCP scenarios (Table D1). Further in the future (2068–2100), the trend is still positive under the RCP4.5 and RCP8.5 scenarios and slightly negative under the RCP2.6 (see Table D1).

With increasing temperature, the probability of extreme events will increase and events considered extreme today may be the norm under certain future scenarios. Present rare heat waves, such as those in Europe 2003 and the U.S. 1980, will become the norm in around 2070 under the RCP8.5 climate change scenario as evident from the ensemble model median of HWMI (Figures 3c and 3d). The extreme Russian heat wave in 2010, which was detected as the strongest heat wave in the present climate, will be the norm (present value equal to the future ensemble median) at the end of the century under the RCP8.5 scenario, although, it will remain rare (present value outside the interquartile range of the model ensemble) under the other two scenarios (Figure 3b).

Under the RCP8.5 scenario heat waves with a magnitude equal to or greater than the magnitude of the events in 2010, 2003, and 1980 show some probability of occurrence starting from ~2050 (Russia), ~2030 (Europe), and ~2045 (U.S.) (Figures 3b–3d).

The probability of occurrence of an extreme heat wave (HWMI $\geq$ 4, note that in 2010, the average of the HWMI in Russia was greater than 5 with both ERA-I and NCEP-II data sets) has been estimated by counting the number of heat waves in the following three periods of 33 years: 1980–2012, 2020–2052, and 2068–2100 (Figure 4).

A direct comparison between models and the reanalysis can be found in Figures 4a–4c. In this figure we show that the models are not able to represent the number and geographical pattern of heat waves as found in the reanalysis, particularly in Europe and the U.S. The models show extreme heat waves only in South America.

In the near future (2020–2052), the RCP2.6 and RCP4.5 scenarios show very similar results: the frequency of extreme heat waves will increase with at least one extreme heat wave in 33 years in the U.S., Europe, and large parts of Africa and three extreme heat waves in northern South America, some parts of Africa, the U.S., and southern Europe (Figures 4d and 4e).

Under the most severe RCP8.5 scenario, large areas of the U.S., South America, Europe, and Indonesia show more than three heat waves in the period 2020–2052, with one extreme heat wave every 2 years in northern Brazil (Figure 4f). At the end of the century (2068–2100), under the RCP8.5 scenario and in a very large part of the globe, an extreme heat wave will occur at least once every 2 years (more than 15 extreme events in 33 years; see Figure 4i).

Our results are similar to *Sillmann et al.* [2013b] showing that the strongest increase in heat wave duration calculated with the WSDI will occur in tropical regions; however, we detect very high HWMI values also in some extratropical regions as, for example, Greenland and Canada (Figures 4i and 5i), which are not detected in *Sillmann et al.* [2013b] by using the WSDI. This is because the HWMI takes into account not only the duration of a heat wave but also the intensity estimated by weighting the temperature values of a heat wave with respect to the probability distribution of the annual maximum of the reference period (see section 2.3). Under the same scenario (RCP8.5) in northern Latin America, Africa, some parts of the U.S., and southern Europe, very extreme heat waves (HWMI > 8, magnitude comparable with the maximum value of the Russian heat wave in 2010) will occur with the same frequency of the extreme heat waves (HWMI > 4), i.e., once every 2 years (Figure 5).

In contrast, at the end of the century under the RCP2.6 mitigation scenario, the probability of extreme heat waves occurring is almost unchanged compared to the period 2020–2052, indicating that this mitigation scenario may be effective in reducing the impact of climate change (Figures 4d, 4g, 5d, and 5g).

4. Conclusions

In this work we have developed the new climate index HWMI that, by taking into account both heat wave duration and intensity, enables the quantification of the magnitude of heat waves across different time periods and regions of the world.

We have estimated the magnitude of extreme heat waves in the present climate and their projection in a warming world by using reanalysis data and IPCC AR5 model outputs, respectively.

According to the statistics of extremes [*Gumbel*, 1954], "However big floods get, there will always be a bigger one coming," the same could be said for heat waves. By using the HWMI, we have shown that the extreme Russian heat wave in 2010 can still be considered a rare event in the future under the less severe scenarios RCP4.5 and RCP2.6. This heat wave may occur under stationary climate [*Dole et al.*, 2011], and it is difficult to link it to greenhouse gas-induced warming [*Intergovernmental Panel on Climate Change*, 2012]. However, in a warmer future climate, the probability of extreme events, such as those in Russia 2010, Europe 2003, and the U.S. 1980, will increase and events considered rare today may be considered the norm under certain future scenarios. Given the disastrous effects of the 2003 and 2010 events in Europe, and the 2011 and 2012 events in the U.S., these results show that we may be facing a serious risk of adverse impacts over larger and densely populated areas if mitigation strategies for reducing global warming are not implemented.

Appendix A: Cumulative Density Function Estimation

The empirical probability distribution function (EPDF) and the corresponding ECDF based on the annual maxima of the subheat wave unscaled magnitudes are estimated using the kernel density estimator (KDE) [*Silverman*, 1986]. The KDE is a nonparametric method for estimating EPDF and ECDF. Given independent and identically distributed annual maxima of subheat wave unscaled magnitudes, T_1, T_2,…, T_N having the common probability density function $f(T)$, where $N = 30$ is the number of years, the general kernel estimator for f is as follows:

$$\hat{f}_h(T) = \frac{1}{N}\sum_{i=1}^{N} K\left(T - T_i, h\right) \tag{A1}$$

T is the subheat wave unscaled magnitude, K is the kernel function, and h is the smoothing bandwidth. Comprehensive reviews of the kernel smoothing method are available in *Silverman* [1986]. The kernel function K is chosen here to the Gaussian function

$$K(x,\sigma) = \frac{1}{\sigma\sqrt{2\pi}} e^{-\frac{x^2}{2\sigma^2}} \tag{A2}$$

By using the method of *Sheather and Jones* [1991], h is calculated. The values of the ECDF are obtained by integrating the $\hat{f}_h(T)$ as follows:

$$\mathrm{ECDF}(T) = \frac{1}{N}\sum_{i=1}^{N}\int_{-\infty}^{T} K\left(T - T_i, h\right) \mathrm{d}T \tag{A3}$$

Appendix B: Heat Wave Magnitude Scale

Referring to the magnitude values of the heat waves that occurred in the last 33 years, heat wave magnitude is defined for values of the HWMI with the following categories (Figure B1):

≤ 1 Normal $< 2 \leq$ Moderate $< 3 \leq$ Severe $< 4 \leq$ Extreme $< 8 \leq$ Very Extreme $< 16 \leq$ Super Extreme $< 32 \leq$ Ultra Extreme.

The levels of the heat wave magnitude scale are defined on a T63 grid using the ERA-I and NCEP-2 HWMI values. We have calculated at each grid point the number of heat waves with a magnitude greater than a fixed threshold in the present period 1980–2012. Subsequently, we estimate the percentage of the global area that recorded (in the period between 1980 and 2012) at least one heat wave with an HWMI value greater than a fixed threshold (see Figure B1) and define the following categories:

Normal. All the grid points show at least one heat wave with HWMI $\geq$ 1 in 33 years.
Moderate. At least one heat wave with HWMI $\geq$ 2 is detected in 70% of the global area.
Severe. At least one heat wave with HWMI $\geq$ 3 is detected in the 25% of the global area.
Extreme. At least one heat wave with HWMI $\geq$ 4 is detected in 5–10% of the global area.
Very extreme. At least one heat wave HWMI $\geq$ 8 is detected in 0.1–1% of the global area.
Super extreme. HWMI $\geq$ 16.
Ultra Extreme. HWMI $\geq$ 32.

The last two categories are defined arbitrarily; in fact, the maximum HWMI value in the present is lower than 12 (see Table 1), and the percentage of the global area with at least one heat wave with HWMI $\geq$12 is zero. We add these two additional categories in order to detect heat waves under the most drastic IPCC AR5 scenarios.

This scale can be applied to a single grid point or to the HWMI median or mean estimated in a region: for example, the Russian heat wave of 2010 was in median an extreme heat wave (HWMI regional median > 4) with a few locations recording a very extreme magnitude (HWMI > 8) (Figure 2 and Table 1 of the main paper).

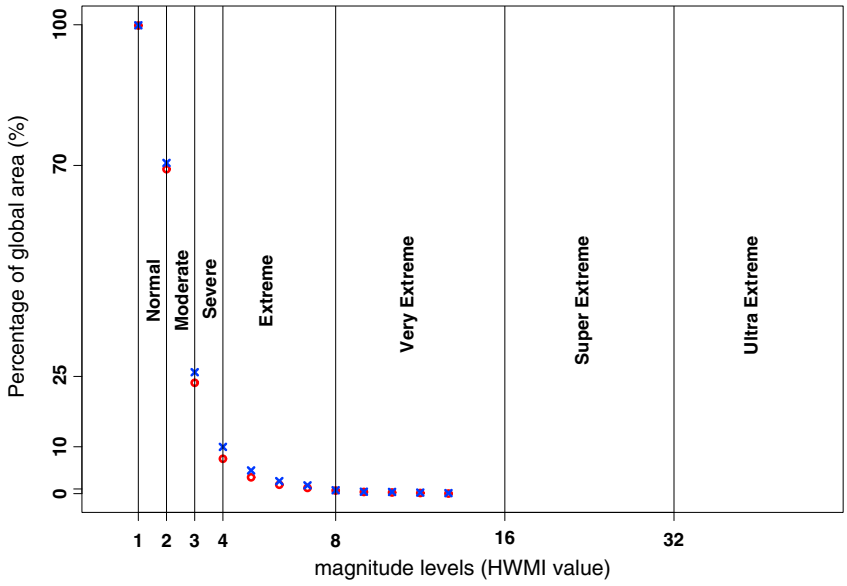

Figure B1. HWMI scale categories. Percentage of global area (*y* axis) with at least one heat wave of a fixed HWMI value (*x* axis) in the period 1980–2012. The blue crosses and red open circles represent the percentage of global area with at least one heat wave of a fixed HWMI value versus the fixed HWMI values calculated with the NCEP-2 and ERA-I data sets, respectively.

Appendix C: List of the CMIP5 Used Models

The HWMI was calculated for daily maximum temperatures from 16 model simulations from the Coupled Model Intercomparison Project Phase 5 (CMIP5) archive (see Table C1).

Table C1. List of the AR5 CMIP5 Used Models

Model	Institution	Spatial Resolution (Longitude × Latitude)
BCC-CSM1-1	Beijing Climate Center, China Meteorological Administration, China	128 × 64 (T42)
CanESM2	Canadian Centre for Climate Modelling and Analysis, Canada	128 × 64 (T42)
CCSM4	National Center for Atmospheric Research, U.S.	288 × 192 (T42)
CNRM-CM5	Centre National de Recherches Meteorogiques, Meteo France, France	256 × 128 (T85) 128 × 64 (T42)
CSIRO-Mk3-6-0	Australian Commonwealth Scientific and Industrial Research Organization, Australia	192 × 96 (T63)
GFDL-ESM2G	Geophysical Fluid Dynamics Laboratory, U.S.	144 × 90
GFDL-ESM2M	Geophysical Fluid Dynamics Laboratory, U.S.	144 × 90
IPSL-CM5A-LR	Institut Pierre-Simon Laplace, France	96 × 96 (T42)
IPSL-CM5A-MR	Institut Pierre-Simon Laplace, France	144 × 143 (T42)
MIROC5	AORI (Atmosphere and Ocean Research Institute), NIES (National Institute for Environmental Studies), JAMSTEC (Japan Agency for Marine-Earth Science and Technology), Japan	256 × 128 (T85)
MIROC-ESM	AORI, NIES, JAMSTEC, Japan	128 × 64 (T42)
MIROC-ESM-CHEM	AORI, NIES, JAMSTEC, Japan	128 × 64 (T42)
MPI-ESM-LR	Max Planck Institute for Meteorology, Germany	192 × 96 (T63)
MPI-ESM-MR	Max Planck Institute for Meteorology, Germany	192 × 96 (T63)
MRI-CGCM3	Meteorological Research Institute, Japan	320 × 160 (T106)
NorESM1-M	Norwegian Climate Centre, Norway	144 × 96 (T42)

Table D1. Nonparametric (Kendall-Tau) Linear Trend (1% Significance Level) of the Yearly Global-Averaged Median for Three Time Windows of 33 Years for Each Single Model, Model Ensemble, and Reanalysis Data

	1980–2012	2020–2052			2068–2100		
	Historical-RCP2.6	RCP2.6	RCP4.5	RCP8.5	RCP2.6	RCP4.5	RCP8.5
Model	($\times 10^{-2}$ HWMI $\times$ yr^{-1})	($\times 10^{-2}$ HWMI $\times$ yr^{-1})			($\times 10^{-2}$ HWMI $\times$ yr^{-1})		
BCC-CSM1-1	1.9	1.0	1.8	3.0	−0.5	0.6	5.8
CanESM2	3.1	1.7	2.1	4.6	0.1	0.6	15.6
CCSM4	2.5	0.8	1.9	2.8	−0.1	0.1	7.2
CNRM-CM5	2.0	1.2	2.7	3.5	−0.5	0.1	10.1
CSIRO-Mk3-6-0	2.2	1.8	3.4	3.9	0.4	0.1	10.1
GFDL-ESM2G	1.5	1.2	1.8	3.0	−0.7	0.3	5.5
GFDL-ESM2M	2.3	0.6	1.5	2.4	−0.3	0.2	5.4
IPSL-CM5A-LR	3.4	1.8	5.1	8.7	−0.0	3.7	3.2
IPSL-CM5A-MR	3.2	2.9	3.6	6.8	−0.7	0.9	2.7
MIROC5	2.3	1.6	2.3	3.1	−0.0	1.4	8.1
MIROC-ESM	1.9	2.3	2.4	3.6	0.2	0.5	16.0
MIROC-ESM-CHEM	1.8	1.8	2.6	3.9	0.1	1.6	16.0
MPI-ESM-LR	1.2	0.8	2.6	3.2	−0.5	0.0	14.0
MPI-ESM-MR	2.4	0.4	2.1	3.4	0.0	0.9	10.9
MRI-CGCM3	1.3	0.2	1.3	1.8	−0.2	0.7	4.4
NorESM1-M	1.6	0.8	1.6	2.6	−0.1	0.5	6.4
Ensemble median	2.1	1.2	2.2	3.3	−0.1	0.7	10.1
Ensemble IQR	0.7	0.9	0.5	0.9	0.5	0.6	6.2
			Reanalysis				
NCEP-2	1.5	-	-	-	-	-	-
ERA-I	2.1	-	-	-	-	-	-

Appendix D: Nonparametric Trend Values

The values of the nonparametric (Kendall-Tau) HWMI global median linear trend for three time windows of 33 years estimated with the models and reanalysis data are reported in Table D1.

Acknowledgments
We acknowledge the World Climate Research Program's Working Group on coupled modeling, which is responsible for CMIP5 model outputs. The data for this paper are available in the CMIP5 archive (http://cmip-pcmdi.llnl.gov/cmip5/data_portal.html). J.S. is supported by the NAPEX project funded through the Norwegian Research Council. Finally, we thank M. Rixen for comments on earlier versions of the manuscript.

References

Alexander, L. V., et al. (2006), Global observed changes in daily climate extremes of temperature and precipitation, *J. Geophys. Res.*, *111*, D05109, doi:10.1029/2005JD006290.

Barriopedro, D., et al. (2011), The hot summer of 2010: Redrawing the temperature record map of Europe, *Science*, *332*, 220–224.

Coumou, D., and S. Rahmstorf (2012), A decade of weather extremes, *Nat. Clim. Change*, *2*, 491–496.

Dee, D. P., et al. (2011), The ERA-Interim reanalysis: Configuration and performance of the data assimilation system, *Q. J. R. Meteorol. Soc.*, *137*, 553–597.

Dole, R., M. Hoerling, J. Perlwitz, J. Eischeid, P. Pegion, T. Zhang, X.-W. Quan, T. Xu, and D. Murray (2011), Was there a basis for anticipating the 2010 Russian heat waves?, *Geophys. Res. Lett.*, *38*, L06702, doi:10.1029/2010GL046582.

Fischer, E. M., and C. Schär (2010), Consistent geographical patterns of changes in high-impact European heatwaves, *Nat. Geosci.*, *3*, 398–403, doi:10.1038/NGEO866.

Frich, P., L. V. Alexander, P. Della-Marta, B. Gleason, M. Haylock, A. Klein Tank, and T. Peterson (2002), Global changes in climatic extremes during the 2nd half of the 20th century, *Clim. Res.*, *19*, 193–212.

Gumbel, E. J. (1954), *Statistical Theory of Extreme Values and Some Practical Applications: Applied Mathematics Series*, vol. 33, U.S. Department of Commerce, National Bureau of Standards, Washington, D. C.

Intergovernmental Panel on Climate Change (2012), *Managing the Risks of Extreme Events and Disasters to Advance Climate Change Adaptation. A Special Report of Working Groups I and II of the Intergovernmental Panel on Climate Change*, edited by C. B. Field et al., 52 pp., Cambridge Univ. Press, Cambridge, U. K., and New York.

Kanamitsu, M., W. Ebisuzaki, J. Woollen, S. K. Yang, J. J. Hnilo, M. Fiorino, and G. L. Potter (2002), NCEP-DOE AMIP-II reanalysis (R-2), *Bull. Am. Meteorol. Soc.*, *83*, 1631–1643.

Kiktev, D., D. M. H. Sexton, L. Alexander, and C. K. Folland (2003), Comparison of modelled and observed trends in indices of daily climate extremes, *J. Clim.*, *16*, 3560–3571.

Meehl, G. A., and C. Tebaldi (2004), More intense, more frequent, and longer lasting heat waves in the 21st century, *Science*, *305*, 994–997.

Min, S.-K., X. Zhang, F. W. Zwiers, and G. C. Hegerl (2011), Human contribution to more-intense precipitation extremes, *Nature*, *470*, 378–381.

Orlowsky, B., and S. Seneviratne (2011), Global changes in extreme events: Regional and seasonal dimension, *Clim. Change*, *110*, 669–696.

Otto, F. E. L., N. Massey, G. J. van Oldenborgh, R. G. Jones, and R. M. Allen (2012), Reconciling two approaches to attribution of the 2010 Russian heat wave, *Geophys. Res. Lett.*, *39*, L04702, doi:10.1029/2011GL050422.

Perkins, S. E., and L. V. Alexander (2012), On the measurement of heat waves, *J. Clim.*, *26*, 4500–4517.

Rousseeuw, P. J., and A. Leroy (1987), *Robust Regression and Outlier Detection*, Wiley Series in Probability and Mathematical Statistics, John Wiley, New York.

Russo, S., and A. Sterl (2011), Global changes in indices describing moderate temperature extremes from the daily output of a climate model, *J. Geophys. Res.*, *116*, D03104, doi:10.1029/2010JD014727.
Schär, C., P. L. Vidale, D. Lüthi, C. Frei, C. Häberli, M. A. Liniger, and C. Appenzeller (2004), The role of increasing temperature variability in European summer heatwaves, *Nature*, *427*, 332–336.
Sheather, S. J., and M. C. Jones (1991), A reliable data-based bandwidth selection method for kernel density-estimation, *J. R. Stat. Soc. Ser. B, Stat. Methodol.*, *53*, 683–690.
Sillmann, J., V. V. Kharin, X. Zhang, F. W. Zwiers, and D. Bronaugh (2013a), Climate extremes indices in the CMIP5 multimodel ensemble: Part 1. Model evaluation in the present climate, *J. Geophys. Res. Atmos.*, *118*, 1716–1733, doi:10.1002/jgrd.50203.
Sillmann, J., V. V. Kharin, F. W. Zwiers, X. Zhang, and D. Bronaugh (2013b), Climate extremes indices in the CMIP5 multimodel ensemble: Part 2. Future climate projections, *J. Geophys. Res. Atmos.*, *118*, 2473–2493, doi:10.1002/jgrd.50188.
Silverman, B. W. (1986), *Density Estimation for Statistics and Data Analysis*, Chapman and Hall, London.
Taylor, K. E., R. J. Stouffer, and G. A. Meehl (2012), An overview of CMIP5 and the experiment design, *Bull. Am. Meteorol. Soc.*, *93*, 485–498.